Article

Reversible Multi-Stimuli Switching of a Spiropyran Functionalized Organic Cage in Solid and Solution

Bijnaneswar Mondal, Aloke Kumar Ghosh, and Partha Sarathi Mukherjee

J. Org. Chem., **Just Accepted Manuscript** • DOI: 10.1021/acs.joc.7b00722 • Publication Date (Web): 05 Jul 2017

Reversible Multi-Stimuli Switching of a Spiropyran Functionalized Organic Cage in Solid and Solution

Bijnaneswar Mondal, Aloke Kumar Ghosh, and Partha Sarathi Mukherjee *

Inorganic and Physical Chemistry Department, Indian Institute of Science, Bangalore-560012, India

ABSTRACT: A spiropyran decorated covalent organic cage (**PC2**) has been designed employing dynamic imine chemistry followed by imine bond reduction. The molecule is capable of altering its colour upon exposure to external stimuli like heat and light. Construction of a 3D organic cage introduces a new piece to the system by swapping of close form to open form in solid state withdiverse colour change. Moreover, this material has high chemical stability and is capable of reversible stimuli-responsive colour change without any degradation for an extended period.

INTRODUCTION

Researchers are fascinated by the materials and systems that can reversibly regulate their structures and properties in reply to environmental stimuli. Stimuli-responsive molecules[1] are capable of changing their structure and/or properties in response to external stimuli like light, heat, pH, etc. Such molecules have drawn attention as key constituents of stimuli-responsive materials, which include self-darkening windows[2], self-healing coatings[3], or silica-based delivery vehicles that can be premeditated to discharge cargo molecules upon activation with a variety of external stimuli.[4] One most common example of molecular switch is spiropyran (**SP**), which is hydrophobic and converts into a highly polar open-ring isomer merocyanine (**MC**) upon exposure to UV light; while the reverse reaction (**MC** to **SP** conversion) can be induced by visible light.[5] Moreover, this reversible isomerization can be promoted by a variety of other external stimuli, such as temperature,[6] acids and bases,[7] redox potential,[8] metal ions[9,10] etc. Among these, light and temperature are two major appealing factors which are environmental friendly in daily use. Due to their tremendous stimuli-response nature, spiropyrans have been extensively studied for use in data storage,[11] chemical sensors,[12] smart materials[13-14] etc.

However, the isomerization process requires a large conformational change in the molecule, which is considered to be an unfavourable step in solid-state. In order to efficiently switch, spiropyran molecules need conformational freedom, which is typically not available within the compactly packed arrays of molecules in the crystalline state. Moreover, as earlier recognized,[15] the metastable **MC** moieties can stabilize each other by interacting via a combination of electrostatic, dipolar, and π–π interactions.[16] This stabilization can favour spontaneous **SP** to **MC** transition when the closed-ring **SP** moieties are brought in local proximity.[17] Though solid state photochromism/thermochromism is more appealing for practical use, simple spiropyran and its derivatives generally show such properties in solution phase mainly. Recently, a few polymers, polyaromatic hydrocarbons and covalent organic frameworks functionalized with spiropyran have been reported to show such properties in solid state as well.[18] Negligible solubility of these materials in common solvents limits their fabrication for practical use. So, it is a grand challenge to harvest materials that will be able to show multi-stimuli responsive character in solution and solid state with proper longevity.

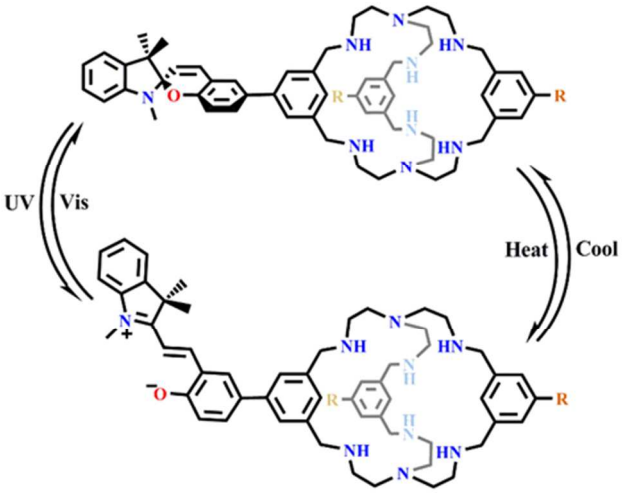

Figure 1. Multi-stimuli reversible isomerization of the close form (**SP**) to open form (**MC**) in cage **PC2**.

In the last few decades, discrete three-dimensional (3D) assemblies have engrossed extensive attention in various ways, either by their beautifully well-designed architectures or by their significant aptitude to act as sensors,[19] catalysts[20] and as molecular hosts.[21] Nevertheless, dynamic covalent chemistry[22] has appeared as an efficient approach for their easy access, which has been established recently in several cage compounds.[23] A smart way to fulfil the conformational freedom constraint would be to render the spiropyran moieties into a pre-designed aldehyde followed by the construction of a 3D architecture. This policy could not only enable efficient isomerization of spiropyran in the solid state, but also helps to upsurge the chemical stability and reversibility using external stimuli (Figure 1).

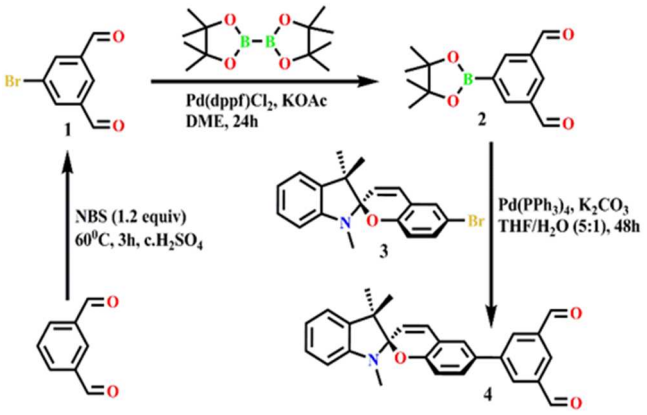

Scheme 1. (a) Synthetic route for the synthesis of spiropyran decorated dialdehyde **4**.

Herein, we report a spiropyran functionalized organic amine cage compound **PC2** (Scheme 2) which is soluble in common organic solvents and exhibits multi-stimuli-responsive properties like photochromism and thermochromism in both solid and solution state in a reversible manner with superior chemical stability for several cycles.

RESULTS AND DISCUSSIONS

Synthesis and characterization of the cage PC2: Reaction of a spiropyran functionalized dialdehyde **4** with a flexible triamine tris(2-aminoethyl)amine (tren) easily yielded discrete organic cage **PC2** in 62% yield. The aldehyde building block **4** was synthesized by palladium catalysed Suzuki-Miyaura cross-coupling reaction between bromo-spiropyran (**3**) and diformylphenylboronic ester (**2**) (Scheme 1). The imine-based cage compound **PC1** was isolated as a yellow solid by treating compound **4** with the triamine 'tren' in 3:2 stoichiometric ratio in chloroform at room temperature for 48 h. The cage **PC1** was converted into more stable amine cage **PC2** by sodium borohydride reduction of the dynamic imine bonds. The as-synthesized **PC2** was characterized by multi-nuclear NMR (^{1}H, ^{13}C), ^{1}H-^{1}H COSY, FT-IR and ESI-MS analyses. In the ESI-MS spectrum (Figure S23), peak at m/z= 1425.8788 corresponding to $[M+H]^{+}$ species unequivocally advocates the formation of [3+2] self-assembled cage. Several efforts to crystallize this cage have so far been unsuccessful.

Photochromism and thermochromism in solution state: Compounds containing spiropyran moieties are well known for their photochromic and thermochromic behaviour. Therefore, organic cage **PC2** decorated with spiropyran in its aromatic backbone shows **SP–MC** isomerization which can be triggered by UV light and heat.

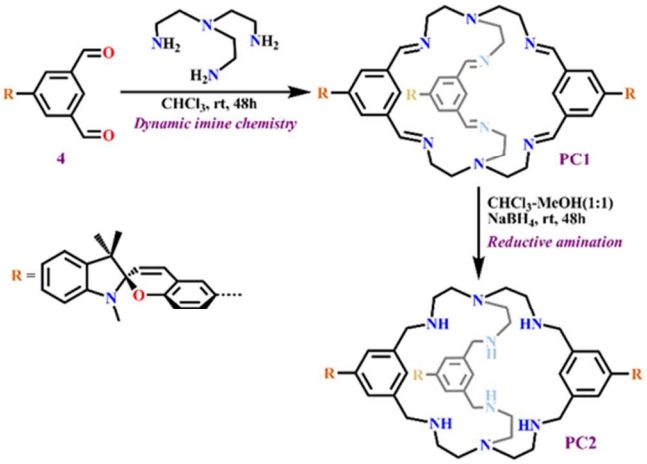

Scheme 2. (a) Synthetic route for the synthesis of organic cage **PC2**.

As can be seen from the UV/Vis absorption of **PC2** in Figure 2, the compound can undergo reversible photoisomerization between their closed-isomer **SP** and open-isomer **SP** under an UV lamp. The absorption peak at 293 nm for the close form of **PC2** decreased and new absorption peaks at 520 and 552 nm assigned to the open form appeared and increased with increased duration of exposure time.

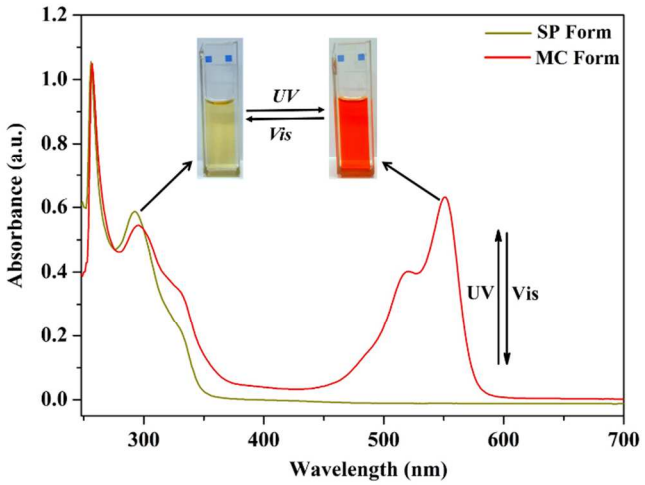

Figure 2. UV/Vis absorption spectra of cage **PC2** (2 mL, 10^{-5} M) in dimethyl sulfoxide recorded under ultraviolet irradiation. The inset shows digital photographs of **SP** and **MC** forms of cage **PC2** in the solution state

In the reverse phenomenon, the peak intensity of the open isomer was gradually decreased over a time period of 2 h under visible light (Figure 3). In view of this fact, the excitation at 520 nm and 552 nm shows the same pattern in the fluorescence spectra suggesting that it is due to the **MC** isomer of the cage (Figure S24). Moreover, the similar thermochromic behaviour is also perceived for cage **PC2** in UV/Vis and fluorescence spectroscopy (Figures S25 and S26) and reversible phenomenon (**MC** form transforms to **SP** form) was taken place by cooling down to room temperature with gradual decolouration (Figure S27).

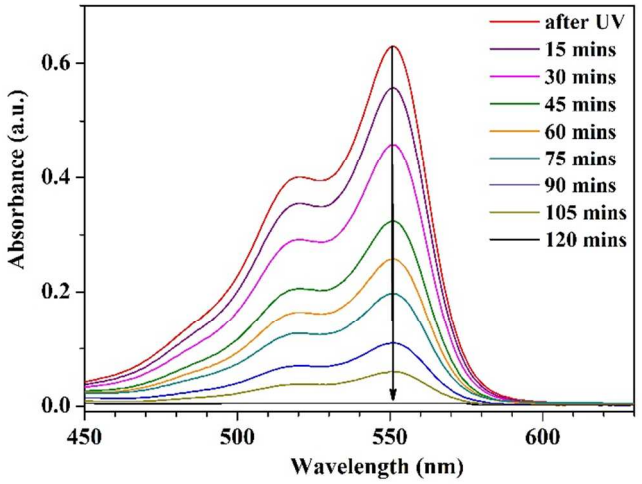

Figure 3. Change in absorption spectra of **MC** form of the cage **PC2** (2 mL, 10^{-5} M) in dimethyl sulfoxide upon exposure to visible light.

Photochromism and thermochromism in solid state:

As discussed earlier colour change due to structural isomerisation of stimuli-responsive materials in their solid state is really challenging for practical applications. Simple spiropyran derivatives generally don't show such structural isomerization in solid state. Similarly, the spiropyran precursor molecules **3** and **4** did not undergo any isomerization in the solid state upon exposure to UV radiation or heating (Figures S32 to S37). Interestingly, the reduced amine cage **PC2** was able to show both photoisomerization and thermoisomerization with a distinct colour change in solid state. The bright yellow colour of **SP** form of the cage gradually turns red **MC** form upon exposure to a UV lamp over a time period of 2.5 h (Figure 4). The reversible phenomenon was observed upon exposure to visible light with gradual decolouration within 2 h (Figure 5). Similarly, solid powder of **PC2** was heated at 80 °C for 2.5 h which converts yellow closed form (**SP** analogue) to red open form (**MC** analogue) (Figures S29 and S30).

As can be seen from the solid-state UV/Vis absorption spectrum of **PC2** in Figure 4, the absorption peak intensity at 293 nm for **SP** form of **PC2** decreased and new absorption peaks at 525 and 563 nm assigned to the open form appeared upon exposure to UV light. In the reverse phenomenon, the peak intensity of the open isomer was gradually decreased over a time period of 2 h under visible light (Figure 5). In view of this fact, the excitation at 525 nm and 563 nm shows a similar pattern in fluorescence spectra suggesting that the **MC** isomer of the cage is formed (Figure S28). Moreover, a similar thermochromic behaviour was also observed for **PC2** in UV/Vis and fluorescence spectroscopy (Figures S29 and S30) and the reversible phenomenon was taken place by cooling down to room temperature over a time period of 2 h (Figure S31). On acidification, the red **MC** isomer transformed to its protonated **MCH**$^+$ form which showed a characteristic band [5j] around 430 nm in UV-Vis spectrum (Figures S51 and S52). Moreover, the **MCH**$^+$ isomer was quite stable for long period under visible light in solid state (Figure S53). Similarly, **MC** to **MCH+** transformation was also observed in heating-cooling cycle upon acidification; and the protonated form was intact for long time at room temperature (Figures S54-S56).

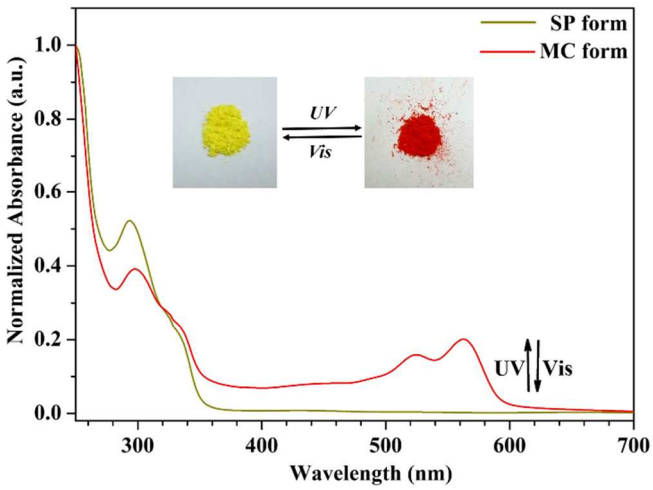

Figure 4. UV/Vis absorption spectra of a thin film of **PC2** recorded under ultraviolet irradiation. The inset shows digital photographs of **SP** and **MC** forms of the cage **PC2** in the solid state.

The precursor compounds **3** and **4** are not able to show isomerisation presumably due to the lack of conformational freedom in compactly crammed arrays of molecules which didn't allow the close-form to open-form transformation in the solid state.

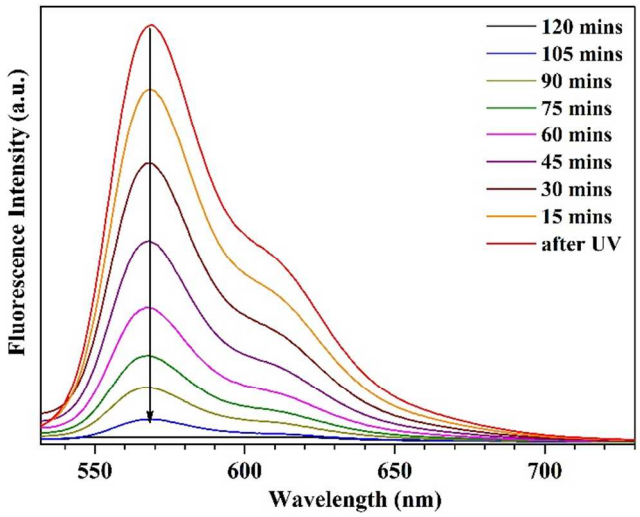

Figure 5. Change in emission spectra of a thin film of cage **PC2** (**MC** analogue) upon exposure to visible light.

Moreover, the chemical stability of compounds **3** and **4** is relatively low under UV radiation or heating for several hours in solid state which is reflected in their UV-Vis spectra (Figures S32, S34, S35 and S37). Whereas in the 3D organic cage architecture (**PC2**), there is enough space for conformational changes. Moreover, very close/dense packing of the larger cage molecules is unlikely due to steric crowding in solid state. Such arrangement of the cage molecules in solid state may lead to loosely packed arrays of molecules with enough intermolecular space for isomerization of **SP**-moiety to **MC**-moiety or *vice versa* to show reversible photochromism and thermochromism.

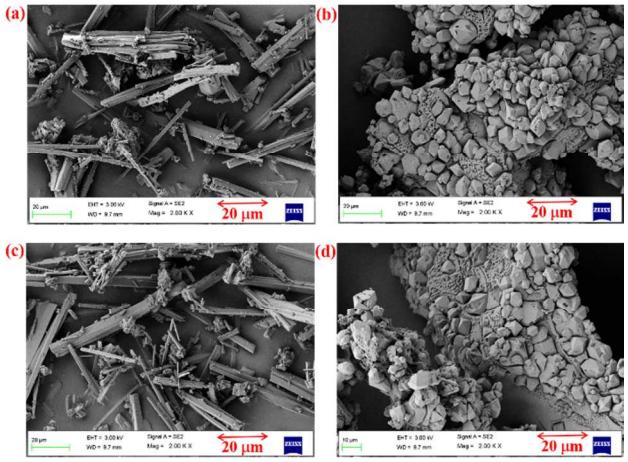

Figure 6. SEM images of cage **PC2** (a) before (b) after UV radiation and (c) before (d) after heating.

Morphology and crystallinity in solid state:

Scanning electron microscopy (SEM) images were taken to investigate the surface morphology of the cage **PC2** in both close and open forms. *'Long rod-shape'* micro-structures were perceived in the **SP** form of cage **PC2**. Whereas, *'random edged'* micro-structures were observed in its open form upon exposure to UV radiation or heat for several hours (Figure 6). A reversible phenomenon is noticed upon the removal of external stimuli where *'random edged'* micro particles are converted into *'long rod-shape'* micro particles. Fortunately, we were also able to get such intermediate images where both kinds of micro-structures were present in a time-dependent experiment (Figure S47, S48 and S49).

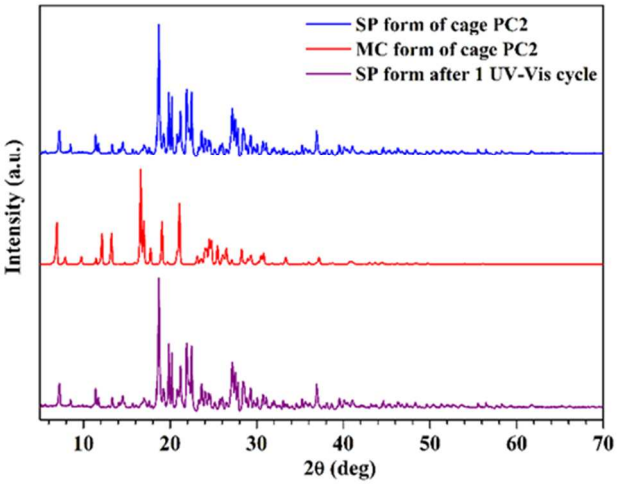

Figure 7. PXRD patterns of cage **PC2** in **SP** form (blue line), **MC** form (red line) and after one UV-Vis cycle (purple line).

PXRD data were collected to check the crystalline nature of the material in both **SP** and **MC** states. High crystalline pattern were observed in PXRD analysis for the **SP**-analogue which was also suggested by the SEM images. We performed a short time (30 min) PXRD analysis for **MC** state as it is reversible in visible light and ambient temperature. Though the scan time period is short, we observed crystalline pattern which is quite different from the **SP** state. After one complete UV-Vis cycle, the material showed PXRD pattern identical to the as-synthesized material (Figure 7) due to reversible nature of the **SP-MC** forms of the cage **PC2**. In DSC thermogram appearance of two small sharp peaks around 80°C suggests that PC2 undergoes phase transition (Figure S50). This result implies that PC2 reversibly converts between two disparate solid-state micro-structures via a phase transition induced by external stimuli.

Reversibility in solution and solid state:

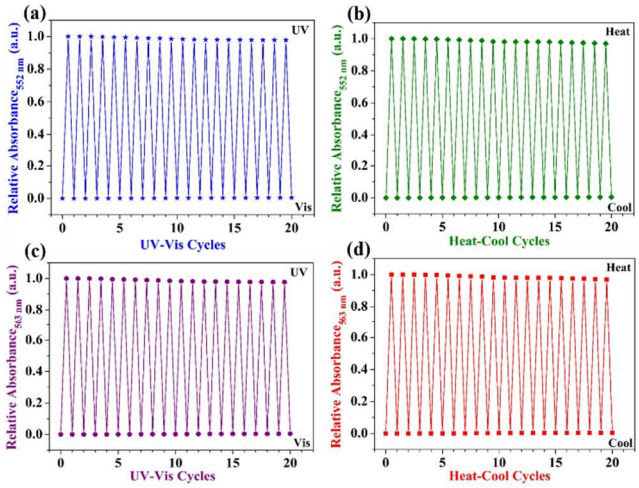

Figure 8. Reversibility of cage **PC2** in solution state upon (a) UV-Vis cycles, (b) heating-cooling cycles; and in solid state upon (c) UV-Vis cycles, (d) heating-cooling cycles.

Reversibility is the crucial factor for practical application of any fatigue free molecular switch with multi-stimuli-responsive nature which makes it more beneficial for its industrial and scientific applications. Moreover, the existence of chemical stability is a vital point for protecting the photochromic dye from environmental deprivation and induces proper longevity. Hence, in order to address this concern in this material (**PC2**), both the solution and solid states were tested for the **SP** to **MC** form and *vice-versa* up to at least twenty consecutive cycles. As portrayed in Figure 8a (Figure S39), experimental results indicate a negligible amount of decrease in absorbance in the solution state. Similar behaviour was also observed in the solid state UV-Vis spectra for at least twenty UV-Vis consecutive cycles (Figure 8c and S43). Both the solution and solid state UV-Vis studies were carried out to check its reversible nature for at least twenty consecutive heating-cooling cycles (Figures S40, S41, S44, and S45). It was found that the absorbance peak of **MC** form of cage **PC2** at 550 nm and 563 nm for solution and solid-states respectively, showed no considerable change in intensity.

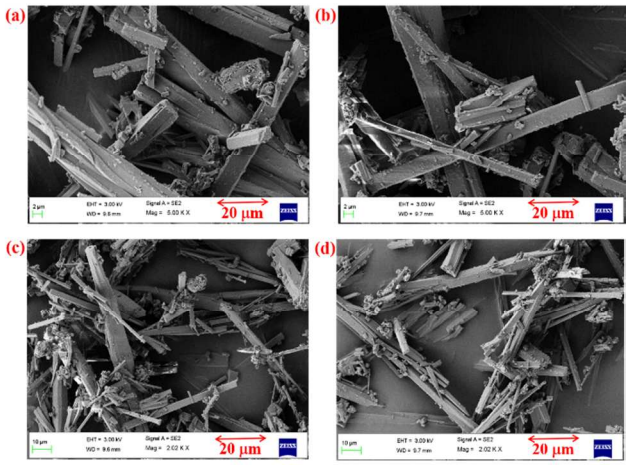

Figure 9. SEM images of cage **PC2** (a) before (b) after 20 UV-Vis cycles; and (c) before (d) after 20 heating-cooling cycles.

The SEM images of the solid **PC2** after twenty cycles also suggested no significant change in the size and morphology of this material (Figure 9). Also to check its reversibility as well as crystallinity in the solid state, PXRD analysis of **SP** form of cage **PC2** was carried out before and after twenty consecutive UV-Vis and heating-cooling cycles (Figure S46). These results further supported the fact that the material retains high chemical stability under several UV-Vis cycles and heating-cooling cycles without any depreciation for an extended period.

CONCLUSION

In summary, we report here a new discrete organic cage compound having spiropyran moieties in its exterior aromatic backbone. The compound shows reversible thermochromism and photochromism. This newly synthesized cage represents a rare example of multi-stimuli responsive reversible molecular switch in both solution and solid states. Photochromism of the compound involves a ring-close to ring-open transformation of the spiropyran moiety. Moreover, this cage compound is sensitive to temperature and shows a reversible distinct colour change upon heating and cooling. These outcomes display the first report on the use of discrete organic cage as a unique model for photochromism and thermochromism in solid state. The simple spiropyran precursor unit doesn't show any photochromism/thermochromism in solid state, while the attachment of this spiropyran unit to a covalent cage leads to conformational isomerisation with distinct colour change in solid state. Reversibility and chemical stability of this cage compound are well retained even after twenty cycles. The material is noteworthy as it is not breeding any photo-fatigue side products; and soluble in common organic solvents. Furthermore, the surface morphology and crystalline patterns are properly investigated for both the close- and open- forms. The present strategy of functionalization of covalent cage with proper functional groups for the generation of solid state stimuli-responsive molecular switch has potential to develop new generation optical switches for practical use.

EXPERIMENTAL SECTION

Materials and methods: Without further purifications, all the chemicals and solvents used for synthesis were purchased from different commercial sources. The NMR spectra were recorded on Bruker 400 MHz instrument. The chemical shifts (**δ**) in the ^{1}H, ^{13}C NMR spectra are accounted in ppm relative to tetramethylsilane (Me_4Si) as an internal standard (0.0 ppm) in $CDCl_3$. High-resolution mass spectra were recorded on a Q-TOF instrument by electrospray ionization (ESI) technique using standard spectroscopic grade solvents. FTIR spectra were recorded on a Bruker ALPHA FTIR spectrometer. Powder X-ray diffraction (PXRD) patterns were recorded on a Phillips PANalytical diffractometer. Scanning electron microscopy (SEM) was performed on a Carl-Zeiss Ultra 55 at an operating voltage of 3-5 kV. Electronic absorption and emission spectra were recorded using a Perkin-Elmer LAMBDA 750 UV-visible spectrophotometer and a HORIBA JOBIN YVON Fluoromax-4 spectrometer respectively. Perkin-Elmer LAMBDA 35 spectrometer and HORIBA JOBIN YVON Fluorolog4 spectrometer were used to record solid state UV-Vis Spectra and Fluorescence Spectra respectively. A Powerstar HQI-BT 400W/D E40 lamp was used for UV radiation with low-temperature equipment and visible light source was a common 75W LED lamp with white light. Analab µ-ThermoCal10 instrument was used for melting point range determination. Thermal characterization was carried out using a PerkinElmer DSC instrument at a heating rate of 1°C/min under a dry nitrogen atmosphere. Elemental analyses (C, H, N) were carried out in a PerkinElmer 240C elemental analyzer.

Synthesis of 1: Compound **1** was prepared according to the literature procedure.[24] ^{1}H NMR ($CDCl_3$, 400 MHz): δ 10.06 (s, 2H), 8.30 (t, J = 1.5 Hz, 1H), 8.26 (d, J = 1.5 Hz, 2H). ^{13}C NMR ($CDCl_3$, 100 MHz): δ 189.6, 138.5, 137.2, 129.3, 124.4. FTIR (cm^{-1}): ν 1685 (C=O).

Synthesis of 2: Compound **1** (1 g, 4.7 mmol), bis(pinacolato)diboron (2.384 g, 9.38 mmol), KOAc (7.370 g, 75.2 mmol) and $Pd(dppf)Cl_2$ (192 mg, 5 mol%) were charged with 60 mL dry 1,2-dimethoxyethane (DME) in a two-neck flask under nitrogen atmosphere. The reaction mixture was degassed and refluxed with stirring under nitrogen atmosphere for 24 h. The reaction was cooled to room temperature and dried under vacuum and extracted with $CHCl_3$ (20 mL ×3). The combined organic phase was washed with brine solution (20 mL ×3) and dried with anhydrous Na_2SO_4. The filtered organic solvent was dried over reduced pressure and the residue was purified by the column chromatography using silica gel and hexane to obtain white compound **2**. Isolated yield: 85% (1039 mg, 4 mmol). Melting point range: (102-104 °C); ^{1}H NMR ($CDCl_3$, 400 MHz): δ 10.12 (s, 2H), 8.55 (d, J = 1.5 Hz, 2H), 8.45 (t, J = 1.5 Hz, 1H), 1.37 (s, 12H). ^{13}C NMR ($CDCl_3$, 100 MHz): δ 191.4, 141.4, 136.4, 132.2, 84.8, 24.9. HRMS (ESI-TOF) m/z: $[M+H]^+$ Calcd for $C_{14}H_{17}BO_4$ 261.1298; Found 261.1292. FTIR (cm^{-1}): ν 1689 (C=O).

Synthesis of 3: Compound **3** was prepared according to the literature procedure.[25] ^{1}H NMR ($CDCl_3$, 400 MHz): δ 7.21–7.16 (m, 3H), 7.08 (d, J = 7.3 Hz, 1H), 6.87 (t, J = 7.3 Hz, 1H), 6.79 (d, J = 10.3 Hz, 1H), 6.60 (d, J = 9.3 Hz, 1H), 6.54 (d, J = 7.6 Hz, 1H), 5.74 (d, J = 10.3 Hz, 1H), 2.72 (s, 3H), 1.30 (s, 3H), 1.17 (s, 3H). ^{13}C NMR ($CDCl_3$, 100 MHz): δ 153.6, 148.1, 136.6, 132.3, 129.2, 128.5, 127.8, 121.6, 120.8, 119.4, 116.9, 111.9, 106.9, 104.6, 52.0, 29.0, 25.9, 20.2. HRMS (ESI-TOF) m/z: $[M+H]^+$ Calcd for $C_{19}H_{18}NOBr$ 356.0650; Found 356.0635.

Synthesis of 4: In a 250 mL double-neck round-bottom flask, 355 mg (1 mmol) of compound **2** and 390 mg (1.5 mmol) of compound **3** were taken in 100 mL THF and into that 20 mL aqueous solution of 414 mg (3 mmol) K_2CO_3 was added. The resulting mixture was degassed under nitrogen atmosphere. Then it was cooled down to room temperature followed by addition of 70 mg (5 mol %) of $Pd(PPh_3)_4$ and heated at 70 °C for 48 h. After the reaction was completed, mixture was concentrated under high vacuum and extracted with $CHCl_3$. The organic phase was dried over anhydrous Na_2SO_4 and the filtered organic phase was dried under reduced pressure. The crude product was purified by preparative TLC plates using silica gel as stationary phase and chloroform as eluent to get a bright yellow powder of **4**. Isolated yield: 54% (221 mg, 0.54 mmol). Melting point range: (114-116 °C); ^{1}H NMR ($CDCl_3$, 400MHz): δ 10.04 (s, 2H), 8.29 (s, 1H), 8.25 (s, 2H), 7.18–7.13 (m, 3H), 7.06 (d, *J* = 7.3 Hz, 1H), 6.84 (t, *J* = 7.3 Hz, 1H), 6.78 (d, *J* = 10.3 Hz, 1H), 6.58 (d, *J* = 9.3 Hz, 1H), 6.52 (d, *J* = 7.6 Hz, 1H), 5.74 (d, *J* = 10.3 Hz, 1H), 2.71 (s, 3H), 1.29 (s, 3H), 1.15 (s, 3H). ^{13}C NMR ($CDCl_3$, 100 MHz): δ 189.6, 153.6, 148.1, 138.5, 137.2, 136.6, 132.3, 129.3, 129.1, 128.4, 127.7, 124.4, 121.6, 120.8, 119.4, 116.9, 111.8, 106.9, 104.6, 51.9, 28.9, 25.9, 20.2. HRMS (ESI-TOF) m/z: $[M+H]^+$ Calcd for $C_{27}H_{23}NO_3$ 410.1756; Found 410.1757. FTIR (cm^{-1}): *ν* 1606 (C=O).

Synthesis of PC1: In a 250 mL round bottom flask, 50 mL $CHCl_3$ solution of tris(2-aminoethyl)amine (24 mg, 0.16 mmol) was added slowly to a stirring solution of aldehyde **4** (100 mg, 0.24 mmol) dissolved in 100 mL $CHCl_3$. The resulting reaction mixture was stirred at room temperature for 48 h. After completion of the reaction, solvent was removed and the obtained deep yellow solid was washed with CH_3OH several times. Isolated yield: 68% (78 mg, 0.05 mmol). Melting point range: (124-126 °C); ^{1}H NMR ($CDCl_3$, 400MHz): δ 8.34 (s, 6H), 7.54 (s, 6H), 7.21–7.16 (m, 9H), 7.08 (d, *J* = 7.3 Hz, 3H), 6.86 (t, *J* = 7.3 Hz, 3H), 6.79 (d, *J* = 10.3 Hz, 3H), 6.60 (d, *J* = 9.4 Hz, 3H), 6.53 (d, *J* = 7.6 Hz, 3H), 5.73 (d, *J* = 10.3 Hz, 3H), 5.41 (s, 3H), 3.79-3.32 (br d, 12H), 2.94-2.72 (br d, 12H), 2.72 (s, 9H), 1.30 (s, 9H), 1.17 (s, 9H). ^{13}C NMR ($CDCl_3$, 100 MHz): δ 158.9, 153.6, 148.1, 138.8, 136.6, 132.3, 130.1, 129.1, 128.5, 127.8, 124.1, 121.6, 120.8, 120.7, 119.4, 116.9, 111.8, 106.9, 104.6, 59.9, 55.7, 51.9, 29.0, 25.9, 20.2. HRMS (ESI-TOF) m/z: $[M+H]^+$ Calcd for $C_{93}H_{93}N_{11}O_3$ 1413.7575; Found 1413.7582, $[M+2H]^{2+}$ Calcd 707.3826; Found 707.3844. FTIR (cm^{-1}): *ν* 2871, 2808, 1641 (CH=N), 1563, 1429, 1333, 1292, 1254, 1155, 1066, 1029, 921, 883, 804, 744, 675, 558.

Synthesis of PC2: 180 mg (0.12 mmol) of **PC1** was taken with 150 mL $CHCl_3$-MeOH (1:1, v/v) binary solvent mixture in a 250 mL round bottom flask. Into this reaction mixture, 58 mg (1.53 mmol) of $NaBH_4$ was added portion wise at room temperature and stirred for 48 h. After completion of the reaction, the solvent was completely removed and the product was extracted in $CHCl_3$. The organic part was washed several times with water and dried over Na_2SO_4 followed by removal of solvent to get a pale yellow solid. Isolated yield: 62% (112 mg, 0.07 mmol). Melting point range: (126-127 °C); ^{1}H NMR ($CDCl_3$, 400MHz): δ 7.40 (s, 6H), 7.19–7.15 (m, 9H), 7.06 (d, *J* = 7.2 Hz, 3H), 6.85 (s, 3H), 6.83 (t, *J* = 7.3 Hz, 3H), 6.78 (d, *J* = 10.3 Hz, 3H), 6.59 (d, *J* = 9.3 Hz, 3H), 6.52 (d, *J* = 7.6 Hz, 3H), 5.72 (d, *J* = 10.3 Hz, 3H), 3.56 (s, 12H), 2.71 (s, 9H), 2.63-2.62 (d, *J* = 5.1 Hz, 24H), 1.29 (s, 9H), 1.15 (s, 9H). ^{13}C NMR ($CDCl_3$, 100 MHz): δ 153.6, 148.1, 143.1, 136.6, 132.3, 129.0, 128.4, 127.7, 125.5, 122.5, 121.6, 120.8, 120.7, 119.4, 116.9, 111.8, 106.9, 104.6, 55.4, 53.2, 51.9, 47.9, 28.9, 25.9, 20.2. HRMS (ESI-TOF) m/z: $[M+H]^+$ Calcd for $C_{93}H_{105}N_{11}O_3$ 1425.8514; Found 1425.8525. FTIR (cm^{-1}): *ν* 3296, 2813, 1568, 1442, 1324, 1198, 1131, 1050, 983, 922, 867, 818, 780, 680, 635. Anal. Calcd for $C_{93}H_{105}N_{11}O_3$: C, 78.39; H, 7.43; N, 10.81. Found: C, 78.41; H, 7.41; N, 10.84.

Sample preparation for solution state UV-Vis and fluorescence spectroscopy: To prepare a 10^{-3} (M) stock solution, 14.24 mg of **PC2** was added to a 10 mL DMSO and stirred for few minutes to obtain a clear yellow solution (**SP** form) at room temperature. In a quartz cuvette, 1980 µl of DMSO and 20 µl of stock solution was added to get a 2 mL of 10^{-5} (M) solution. This solution was used for UV-Vis spectrum analysis. Then it was irradiated for 2 hours with UV light to get a red solution (**MC** form) and measured the UV-Vis spectrum immediately. This method was repeated to check reversibility upto 20 UV-Vis cycles. The same method was repeated for heating-cooling cycle and to check reversibility for 20 cycles. For recording fluorescence spectrum, the same method was used for making 10^{-5} (M) solution of **PC2** in DMSO. Then emission spectra of the **MC** form of **PC2** were recorded by the excitation at 520 and 552 nm.

Sample preparation for solid state UV-Vis and fluorescence spectroscopy: In a typical stock solution preparation, 20 mg of **PC2** was dissolved in 2 mL of DMSO. A few drops of this solution were placed on a clean quartz plate to make an ultra-thin film by spin coating method. This thin film was used to measure solid state UV-Vis spectrum. Then it was irradiated for 2.5 hours with UV light and then again UV-Vis spectrum was recorded immediately. This thin film was used to check reversibility upto 20 UV-Vis cycles. The same method was repeated for heating-cooling and used for 20 cycles to check reversibility. For fluorescence spectrum, the same method was used for making thin film of **PC2** on a quartz plate. Then emission spectra of the **MC** form of cage **PC2** were recorded by the excitation at 525 and 563 nm.

Sample preparation for solid state UV-Vis spectroscopy upon acidification: In a typical stock solution preparation, 14.2 mg of **PC2** was dissolved in 1 mL of DMSO. This solution was coated on a clean quartz plate to make a thin film by spin coating method. This thin film (**PC2-SP**) was used to record it's solid state UV-Vis spectrum. Then it was irradiated for 2.5 hours with UV light and then again UV-Vis spectrum was recorded immediately (**PC2-MC**). 10 equivalents of HCl was added on this and colour changed from red to pinkish (**PC2-MCH$^+$**). Then again it was recorded for UV-Vis spectrum. After keeping this plate under visible light for 6h, UV-Vis spectrum was recorded. The same method was followed during heating-cooing cycle upon acidification.

Sample preparation for Scanning Electron Microscopy (SEM) analysis: Yellow (**SP** form) solid sample (1 mg) was placed on a carbon tape and SEM analysis was done. Red coloured (**MC** form) solid sample (1 mg) was placed on a carbon tape immediately after the UV radiation and then SEM analysis was done to check the morphology. For reversibility check, after 20 consecutive UV-Vis cycles, the yellow coloured (**SP** form) material was placed on carbon tape and SEM

analysis was carried out. The same method was followed for heating-cooling cycles to check the reversibility. To get intermediate images, first **SP** form was converted to **MC** form by UV radiation; then this material was placed under visible light for 20 min and immediately placed on a carbon tape for SEM analysis. For heating-cooling cycle, the same procedure was followed where it was kept for 20 min at room temperature. All the SEM analyses were carried out at 22°C which does not have that much effect on the conversion time of **MC** to **SP** form.

Sample Preparation for PXRD analysis: As-synthesized yellow (**SP** form) cage **PC2** was placed on a flat silicon plate and PXRD was carried out. This material was irradiated with UV light to convert into **MC** form (red colour) and immediately PXRD was carried out for 30 min. After coming to its **SP** form, the same material was again used for PXRD analysis to check crystallinity. To check its chemical stability and crystallinity after twenty consecutive UV-Vis and heating-cooling cycles, the material was used for PXRD analysis. Then it was compared with PXRD patterns of as-synthesized material.

ASSOCIATED CONTENT

^{1}H, ^{13}C and ^{1}H-^{1}H COSY NMR of the compounds, PXRD, SEM and ESI-MS, FTIR, UV/Vis, fluorescence spectra of the cage compound. This material is available free of charge via the Internet at http://pubs.acs.org.

AUTHOR INFORMATION

Corresponding Author

* E-mail: psm@ipc.iisc.ernet.in.

Notes

The authors declare no competing financial interest.

ACKNOWLEDGMENT

P. S. M. is grateful to DST-New Delhi (India) for Swarnajayanti Fellowship (DST/SJF/2012/CS1). B. M. acknowledges the CSIR (New Delhi) for research fellowship. A.K.G. is grateful to UGC (India) for Dr. D. S. Kothari Postdoctoral fellowship. We are thankful to Mr. Abhisek Mahapatra for solid state UV-Vis and fluorescence spectral analysis and Mr. Rupak Saha for PXRD data collection. We are also thankful to Ms. Saheli Chakrabarty for DSC experiment.

ABBREVIATIONS

REFERENCES

(1) Feringa, B. L.; Browne, W. R. *Molecular Switches*, Wiley-VCH, 2011.

(2) McCarthy, W. R.; Powers, M. US Patent 20110102878 A1 filed 29 October 2010, issued 5 May 2011.

(3) (a) Burnworth, M.; Tang, L.; Kumpfer, J. R.; Duncan, A. J.; Beyer, F. L.; Fiore, G. L.; Rowan, S. J.; Weder, C. *Nature*, **2011**, *472*, 334–337. (b) Ito, K. *Curr. Opin. Solid State Mater. Sci*. **2010**, *14*, 28–34. (c) Ito, K.; Araki, J.; Suzuki, T.; Yamanaka, M.; Watanabe, K. US Patent 7943718 B2 filed 23 August 2006, issued 17 May 2011.

(4) (a) Cotí, K. K.; Belowich, M. E.; Liong, M.; Ambrogio, M. W.; Lau, Y. A.; Khatib, H. A.; Zink, J. I.; Khashab, N. M.; Stoddart, J. F. *Nanoscale*, **2009**, *1*, 16–39. (b) Li, Z. X.; Barnes, J. C.; Bosoy, A.; Stoddart, J. F.; Zink, J. I. *Chem. Soc. Rev*. **2012**, *41*, 2590–2605.

(5) (a) Berkovic, G.; Krongauz, V.; Weiss, V. *Chem. Rev.* 2000, **100**, 1741–1753. (b) Minkin, V. I. *Chem. Rev.* **2004**, *104*, 2751–2776. (c) Andersson, J.; Li, S.; Lincoln, P.; Andreasson, J. *J. Am. Chem. Soc*. **2008**, *130*, 11836–11837. (d) Buback, J.; Kullmann, M.; Langhojer, F.; Nuernberger, P.; Schmidt, R.; Wurthner, F.; Brixner, T. *J. Am. Chem. Soc.* **2010**, *132*, 16510–16519. (e) Chovnik, O.; Balgley, R.; Goldman, J. R.; Klajn, R. *J. Am. Chem. Soc.* **2012**, *134*, 19564–19567. (f) Klajn, R.; Bishop, K. J.; Fialkowski, M.; Paszewski, M.; Campbell, C. J.; Gray, T. P.; Grzybowski, B. A. *Science* **2007**, *316*, 261–264. (g) Maity, C.; Hendriksen, W. E.; van Esch, J. H.; Eelkema, R. *Angew. Chem. Int. Ed*. **2015**, *54*, 998–1001. (h) Liu, Z.; Liu, T.; Lin, Q.; Bao, C.; Zhu, L. *Angew. Chem. Int. Ed.* **2015**, *54*, 174–178. (i) Shiraishi, Y.; Tanaka, K.; Shirakawa, E.; Sugano, Y.; Ichikawa, S.; Tanaka, S.; Hirai, T. *Angew. Chem. Int. Ed.* **2013**, *52*, 8304–8308. (j) Klajn, R. *Chem. Soc. Rev*. **2014**, *43*, 148.

(6) (a) Shiraishi, Y.; Itoh, M.; Hirai, T. *Phys. Chem. Chem. Phys.* **2010**, *12*, 13737–13745. (b) Landgraf, J. K.; Braun, M.; Özcoban, C.; Goncalves, D. P. N.; Heckel, A.; Wachtveitl, J. *J. Am. Chem. Soc*. **2012**, *134*, 14070–14077. (c) Chen, J.-R.; Yang, D.-Y. *Org. Lett.* **2009**, *11*, 1769–1772. (d) Shiraishi, Y.; Miyamoto, R.; Hirai, T. *Org. Lett.* **2009**, *11*, 1571–1574.

(7) (a) Doron, A.; Katz, E.; Tao, G.; Willner, I. *Langmuir*, **1997**, *13*, 1783 – 1790. (b) Kong, L.; Wong, H. L.; Tam, A. Y. Y.; Lam, W. H.; Wu, L.; Yam, V. W. W. *ACS Appl. Mater. Interfaces* **2014**, *6*, 1550 – 1562. (c) Xie, X.; Mistlberger, G.; Bakker, E. *J. Am. Chem. Soc.* **2012**, *134*, 16929 – 16932. (d) Remon, P.; Li, S. M.; Grøtli, M.; Pischel, U.; Andreasson, J. *Chem. Commun.*, **2016**, *52*, 4659 – 4662.

(8) (a) Kortekaas, L.; Ivashenko, O.; van Herpt, J. T.; Browne, W. R. *J. Am. Chem. Soc*. **2016**, *138*, 1301 – 1312. (b) Kumar, S.; van Herpt, J. T.; Gengler, R. Y. N.; Feringa, B. L.; Rudolf, P.; Chiechi, R. C. *J. Am. Chem. Soc*., **2016**, *138*, 12519 – 12526.

(9) (a) Wojtyk, J. T.C.; Buncel, E.; Kazmaier, P. M. *Chem. Commun.*, **1998**, 1703 – 1704. (b) Fries, K.; Samanta, S.; Orski, S.; Locklin, J. *Chem. Commun.*, **2008**, 6288 – 6290. (c) Guo, X.; Zhang, D.; Tao, H.; Zhu, D. *Org. Lett.*, **2004**, *6*, 2491 – 2494. (d) Guo, Z.-Q.; Chen, W.-Q.; Duan, X.-M. *Org. Lett.*, **2010**, *12*, 2202 – 2205.

(10) (a) Sagara, Y.; Kato, T. *Nat. Chem.* **2009**, *1*, 605 – 610. (b) Lee, C. K.; Davis, D. A.; White, S. R.; Moore, J. S.; Sottos, N. R.; Braun, P. V. *J. Am. Chem. Soc.* **2010**, *132*, 16107 – 16111. (c) Zhang, H.; Gao, F.; Cao, X.; Li, Y.; Xu, Y.; Weng, W.; Boulatov, R. *Angew. Chem. Int. Ed.* **2016**, *55*, 3040 – 3044.

(11) (a) Guo, X.; Zhang, D.; Zhu, D. *Adv. Mater.* **2004**, *16*, 125 – 130. (b) Raymo, F. M.; Alvarado, R. J.; Giordani, S.; Cejas, M. A. *J. Am. Chem. Soc*. **2003**, *125*, 2361 – 2364. (c) Zhu, L.; Zhu, M.-Q.; Hurst, J. K.; Li, A. D. Q. *J. Am. Chem. Soc.* **2005**, *127*, 8968 – 8970. (d) Giordani, S.; Raymo, F. M. *Org. Lett.* **2003**, *5*, 3559 – 3562. (e) Tomozaki, K.; Mihara, H. *J. Am. Chem. Soc.* **2007**, *129*, 8345–8352. (f) Nagashima, S.; Murata, M.; Nishihara, H. *Angew. Chem. Int. Ed.* **2006**, *45*, 4298–4301. (g) Raymo, F. M.; Giordani, S. *Org. Lett.*, **2001**, *3*, 3475 – 3478.

(12) (a) Shao, N.; Zhang, Y.; Cheung, S.; Yang, R.; Chan, W.; Mo, T.; Li, K.; Liu, F. *Anal. Chem.* **2005**, *77*, 7294 – 7303. (b) Li, Y.; Duan, Y.; Li, J.; Zheng, J.; Yu, H.; Yang, R. *Anal. Chem.* **2012**, *84*, 4732 – 4738. (c) Champagne, B.; Plaquet, A.; Pozzo, J.-L.; Rodriguez, V.; Castet, F. *J. Am. Chem. Soc*. **2012**, *134*, 8101 – 8103.

(13) (a) Setaro, A.; Bluemmel, P.; Maity, C.; Hecht, S.; Reich, S. *Adv. Funct. Mater.* **2012**, *22*, 2425 – 2431. (b) Zhang, M.; Hou, X.; Wang, J.; Tian, Y.; Fan, X.; Zhai, J.; Jiang, L. *Adv. Mater.* **2012**, *24*, 2424 – 2428. (c) Liu, G.; Wang, J. *Angew. Chem. Int. Ed.* **2010**, *49*, 4425 – 4429. (d) Silvi, S.; Arduini, A.; Pochini, A.; Secchi, A.; Tomasulo, M.; Raymo, F. M.; Baroncini, M.; Credi, A. *J. Am. Chem. Soc.* **2007**, *129*, 13378 – 13379. (e) Yildiz, I.; Impellizzeri, S.; Deniz, E.; McCaughan, B.; Callan, J. F.; Raymo, F. M. *J. Am. Chem. Soc.* **2011**, *133*, 871 – 879. (f) Byrne, R.; Diamond, D. *Nat. Mater.* **2006**, *5*, 421 – 424. (g) Kundu, P. K.; Samanta, D.;

Leizrowice, R.; Margulis, B.; Zhao, H.; Börner, M.; Udayabhaskararao, T.; Manna, D.; Klajn, R. *Nat. Chem*. **2015**, *7*, 646 – 652.

(14) (a) Chen, L.; Wu, J.; Schmuck, C.; Tian, H. *Chem. Commun.* **2014**, *50*, 6443 – 6446. (b) Zhu, L.; Wu, W.; Zhu, M.-Q.; Han, J. J.; Hurst, J. K.; Li, A. D. Q. *J. Am. Chem. Soc.* **2007**, *129*, 3524 – 3526. (c) Shao, N.; Jin, J.; Wang, H.; Zheng, J.; Yang, R.; Chan, W.; Abliz, Z. *J. Am. Chem. Soc.* **2010**, *132*, 725 – 736. (d) Özçoban, C.; Halbritter, T.; Steinwand, S.; Herzig, L.-M.; Landgraf, J. K.; Askari, N.; Groher, F.; Fürtig, B.; Richter, C.; Schwalbe, H.; Suess, B.; Wachtveitl, J.; Heckel, A. *Org. Lett.* **2015**, *17*, 1517 – 1520.

(15) (a) Cabrera, I.; Shvartsman, F.; Veinberg, O.; Krongauz, V. *Science* **1984**, *226*, 341–343. (b) Seki, T.; Ichimura, K.; Ando, E. *Langmuir*, **1988**, *4*, 1068–1069. (c) Tachibana, H.; Yamanaka, Y.; Sakai, H.; Abe, M.; Matsumoto, M. *J. Lumin.* **2000**, *87-89*, 800–802. (d) Onai, Y.; Mamiya, M.; Kiyokawa, T.; Okuwa, K.; Kobayashi, M.; Shinohara, H.; Sato, H. *J. Phys. Chem.* **1993**, *97*, 9499–9505.

(16) Klajn, R. *Chem. Soc. Rev.* **2014**, *43*, 148–184.

(17) (a) Goldburt, E.; Shvartsman, F.; Krongauz, V. *Macromolecules*, **1984**, *17*, 1876–1878. (b) Cabrera, I.; Krongauz, V. *Nature*, **1987**, *326*, 582 – 585.

(18) (a) Bénard, S.; Yu, P. *Chem. Commun.*, **2000**, 65–66. (b) Lopez, A. J.; Hernando, J.; Molina, D. R.; Monje, P. G.; Sedo, J.; Roscini, C. *Angew. Chem. Int. Ed.* **2016**, *55*, 1-6. (c) Knittel, T. W.; Krongauz, V. *Macromolecules,* **1985**, *18*, 2124-2126. (d) Kundu, P. K.; Olsen, G. L.; Kiss, V.; Klajn, R. *Nat. Commun.*, **2014**, *5*, 3588 – 3596. (e) Harada, J.; Kawazoe, Y.; Ogawa, K. *Chem. Commun.*, **2010**, *46*, 2593–2595.

(19) (a) Wang, M.; Vajpayee, V.; Shanmugaraju, S.; Zheng, Y.; Zhao, Z.; Kim, H.; Mukherjee, P. S.; Chi, K.-W.; Stang, P. J. *Inorg. Chem.* **2011**, *50*, 1506 – 1512. (b) Dong, J.; Zhou, Y.; Zhang, F.; Cui, Y. *Chem. Eur. J.* **2014**, *20*, 6455 – 6461. (c) Xuan, W.; Zhang, M.; Liu, Y.; Chen, Z.; Cui, Y. *J. Am. Chem. Soc.* **2012**, *134*, 6904 – 6907. (d) Zhang, J.; Li, Y.; Yang, W.; Lai, S.; Zhou, C.; Liu, H.; Chec, C.; Li, Y. *Chem. Commun.* **2012**, *48*, 3602 – 3604. (e) Acharyya, K.; Mukherjee, P. S. *Chem. Commun.* **2014**, *50*, 15788 – 15791.

(20) (a) Murase, T.; Nishijima, Y.; Fujita, M. *J. Am. Chem. Soc.*, **2012**, *134*, 162 – 164. (b) Zhao, C.; Sun, Q.; Hart-Cooper, W. M.; DiPasquale, A. G.; Toste, F. D.; Bergman, R. G.; Raymond, K. N. *J. Am. Chem. Soc.* **2013**, *135*, 18802 – 18805. (c) Zhang, Q.; Tiefenbacher, K. *J. Am. Chem. Soc.* **2013**, *135*, 16213 – 16219. (d) Hart-Cooper, W. M.; Clary, K. N.; Toste, F. D.; Bergman, R. G.; Raymond, K. N. *J. Am. Chem. Soc.* **2012**, *134*, 17873 – 17876. (e) Mondal, B.; Acharyya, K.; Howlader, P.; Mukherjee, P. S. *J. Am. Chem. Soc.* **2016**, *138*, 1709 – 1716. (f) Sun, J-K.; Zhan, W-W.; Akita, T.; Xu, Q. *J. Am. Chem. Soc.*, **2015**, *137*, 7063 – 7066.

(21) (a) Zhang, K.; Ajami, D.; Gavette, J. V.; Rebek, J. *J. Am. Chem. Soc.* **2014**, *136*, 5264 – 5266. (b) Wang, W.; Wanga, Y. -X.; Yang, H.-B. *Chem. Soc. Rev*., **2016**, *45*, 2656-2693. (c) Wei, P.; Yan, X.; Huang, F. *Chem. Soc. Rev*., **2015**, *44*, 815 – 832. (d) Zhang, M.; Yan, X.; Huang, F.; Niu, Z.; Gibson, H. W. *Acc. Chem. Res.*, **2014**, *47*, 1995 – 2005.

(22) (a) Cougnon, F. B. L.; Sanders, J. K. M. *Acc. Chem. Res.* **2012**, *45*, 2211 – 2221. (b) Rowan, S. J.; Cantrill, S. J.; Cousins, G. R. L.; Sanders, J. K. M.; Stoddart, J. F. *Angew. Chem., Int. Ed.* **2002**, *41*, 898 – 952. (c) Reek, J. N. H.; Otto, S. Dynamic Combinatorial Chemistry, Wiley-VCH, Weinheim, 2010. (d) Lehn, J. M. *Chem. Eur. J.* **1999**, *5*, 2455 – 2463.

(23) (a) Mitra, T.; Jelfs, K. E.; Schmidtman, M.; Ahemed, A.; Chong, S. Y. D.; Adams, J.; Cooper, A. I. *Nat. Chem.* **2013**, *5*, 276 – 281. (b) Jiang, S.; Jelfs, K. E.; Holden, D.; Hasell, T.; Chong, S. Y.; Haranczyk, M.; Trewin, A.; Cooper, A. I. *J. Am. Chem. Soc.* **2013**, *135*, 17818 – 17830. (c) Zhang, G.; Presly, O.; White, F.; Oppel, I. M.; Mastalerz, M. *Angew. Chem., Int. Ed.* **2014**, *53*, 5126 – 5130. (d) Ding, H.; Yang, Y.; Li, B.; Pan, F.; Zhu, G.; Zeller, M.; Yuan, D.; Wang, C. *Chem. Commun*. **2015**, *51*, 1976 – 1979.

(24) Blackburn, O. A.; Coe, B. J.; Helliwell, M.; Raftery, J. *Organometallics*, **2012**, *31*, 5307 – 5320.

(25) Qi, Q.; Qian, J.; Ma, S.; Xu, B.; Zhang, S. X.; Tian, W. *Chem. Eur. J.* **2015**, *21*, 1149 – 1155.

Insert Table of Contents artwork here